View Online
Dynamic Article Links

Dalton Transactions

Cite this: *Dalton Trans.*, 2011, **40**, 9580

www.rsc.org/dalton

PAPER

Pharmaceutical formulation affects titanocene transferrin interactions†

Katherine M. Buettner, Robert C. Snoeberger III, Victor S. Batista and Ann M. Valentine*‡

Received 30th April 2011, Accepted 10th June 2011
DOI: 10.1039/c1dt10805k

Since the discovery of the anticancer activity of titanocene dichloride (TDC), many derivatives have been developed and evaluated. MKT4, a soluble, water-stable formulation of TDC, was used for both Phase I and Phase II human clinical trials. This formulation is investigated here by using ^{1}H and ^{13}C NMR, FT-ICR mass spectrometry, and UV/vis-detected pH-dependent speciation. DFT calculations are also utilized to assess the likelihood of proposed species. Human serum transferrin has been identified as a potential vehicle for the Ti anticancer drugs; these studies examine whether and how formulation of TDC as MKT4 may influence its interactions, both thermodynamic and kinetic, with human serum transferrin by using UV/vis absorption and fluorescence quenching. MKT4 binds differently than TDC to transferrin, showing different kinetics of binding as well as a different molar absorptivity of binding (7500 M^{-1} cm^{-1} per site). Malate, used in the buffer for MKT4 administration, acts as a synergistic anion for Ti binding, shifting the tyrosine to Ti charge transfer energy and decreasing the molar absorptivity to 5000 M^{-1} cm^{-1} per site. These differences may have had consequences after the change from TDC to MKT4 in human clinical trials.

Introduction

Titanium coordination compounds have been studied since the 1970s for their anticancer activity and shown promising *in vitro* activity against many cancer cell lines.[1–14] One of the best studied complexes, both for its anticancer activity and its reactivity in water, is titanocene dichloride (TDC).[12]

Titanocene dichloride exhibited strong activity against ovarian, cervical and colon cancer cell lines.[3,5,15,16] A formulation of TDC went through two Phase I[17,18] and two Phase II clinical trials,[19,20] but was determined to have dose-limiting toxicity and has not been further tested. Although most of the preclinical studies were performed with TDC, usually administered in a 10% DMSO solution, the reagent used in the human clinical trials was a soluble, water stable formulation known as MKT4.[17–20] This formulation was prepared by combining TDC and excess mannitol with sodium chloride in water, and lyophilizing this mixture to dryness.[21] It was administered in a low pH malic acid buffer.[17–20]

One reason that this polyol formulation was used is that TDC itself is prone to hydrolysis and hydrolytic precipitation, which ultimately produces insoluble, inactive species with the empirical formula $TiCp_{0.31}O_{0.30}(OH)$ (Cp = cyclopentadienyl).[22] The hydrolysis of TDC is affected by the presence of metal binding ligands in solution, including proteins.[23]

Serum transferrin (Tf) has been identified as a possible carrier for Ti(IV) in human serum.[24,25] This notion is supported by the high concentration of Tf in serum (35 μM),[26] the binding of many nonferrous metals to Tf,[27] as well as the observation of Ti bound to Tf *in vivo*.[28] The selectivity of Ti for cancer cells may be related to the increased number of Tf receptors on the surface of those cells compared to healthy cells,[29–31] and the low levels of fully iron-saturated Tf in serum.[32] It is still not clear whether Tf is the delivery vehicle for the therapeutic fraction of Ti from the bioactive compounds, or whether this binding is a side reaction that decreases their efficacy. Co-administration of Tf with Ti compounds decreases their potency in at least some assays.[33] Either way, the interactions of Tf with these complexes are likely to be important to their bioactivity.

Two equiv of Ti(IV) bind to Tf, and this binding can be monitored by UV/vis changes at 241, 295 and 321 nm.[24] The absorbance at 321 nm is a characteristic tyrosine to Ti(IV) charge transfer band. Binding has been further characterized by using Ti citrate, TDC and some of its derivatives, and Ti nitrilotriacetate.[24,34–40] The extinction coefficients for Ti(IV)-bound Tf can vary. One hypothesis, supported by small molecule models, holds that unhydrolyzed Ti (Ti having no water-derived ligands such as hydroxo- or oxo- ligands) in the Tf binding site exhibits an extinction coefficient at 321 nm of 9–10 000 M^{-1} cm^{-1} for each Ti(IV) site, while hydrolyzed forms exhibit lower extinction coefficients.[24,34,35,37,41] Titanocene dichloride binds to Tf with a molar absorptivity of 2500 M^{-1} cm^{-1} per Tf binding site at 321 nm.[25]

The differences in Tf binding among different complexes of Ti(IV) raise questions about MKT4. MKT4 was frequently treated as if it were equivalent to TDC,[17–20] but it is not clear to what degree formulation affects solution speciation.

Yale University, New Haven, CT, 06520-8107, USA

† Electronic supplementary information (ESI) available: ^{1}H NMR of MKT4, TDC batch titration, TDC_{DMSO} binding data, fluorescence spectra, computational data and structures, absorbance profiles of Tf binding data, and models spectra from kinetic fits. See DOI: 10.1039/c1dt10805k

‡ Current address: Temple University, Philadelphia, PA, 19122, USA. E-mail: ann.valentine@temple.edu

Table 1 A comparison of IC_{50} values determined for both MKT4 and TDC. All values are listed in μM. A549 cells are human lung carcinoma cells, A2780 cells are human ovarian cancer cells, and A2780/CP cells are the cisplatin resistant variation of those cells. The HeLa cell line is a line of cervical cancer cells

Cell line	MKT4	TDC
A549	129–>200[42]	168[43]
A2780	109–>200[42,44]	570[16]
A2780/CP	>200[42,45]	600[46]
HeLa	>200[42,45]	424[13]

Direct comparison of TDC and MKT4 cytotoxicity was made in only a few lung, ovarian and cancer cell lines. MKT4 was often listed as above a threshold for activity, so quantitative comparisons between MKT4 and TDC cannot be made for most of the cell lines. Table 1 shows the cell lines for which both TDC and MKT4 IC_{50} values are available.[13,16,42–46] Titanocene dichloride showed somewhat higher activity *in vivo* than it did *in vitro*.[7]

In order to evaluate better the outcome of the clinical trials that used MKT4, it is important to characterize more fully MKT4 and determine how it may interact with Tf. In this work, the properties of MKT4 are explored by using NMR, mass spectrometry and UV/vis spectroscopy, supported by calculations. The differences between MKT4 and TDC were further studied by investigating their interactions with Tf. The conditions used for the clinical trials of TDC were mimicked in order to understand more completely the Tf binding that might have been taking place during the clinical trials.

Experimental

Materials

All solutions were prepared with nanopure water (18.2 MΩ·cm resistivity; Barnstead model D11931 water purifier). Titanocene dichloride was purchased from Aldrich and prepared fresh; for samples which were going to be raised above pH 5, 10% DMSO was required in the buffer. Human serum apotransferrin was obtained from Sigma. Its purity was checked by SDS-PAGE and its iron-free status was verified by UV/vis. D-Mannitol was purchased from Fisher and used as received. All other materials were of high purity and used as received.

Instrumentation

UV/vis experiments were performed by using a Varian Cary 50 spectrophotometer. Fluorescence experiments were performed by using a Shimadzu RF-5301 PC spectrofluorophotometer.

MKT4 characterization

The patent describing MKT4 covers formulation with a variety of polyols.[21] In the formulation used for the clinical trials, MKT4 was prepared by combining 100 mg TDC with a seven-fold molar excess of mannitol (500 mg) and a nineteen fold molar excess of sodium chloride (450 mg) in 50 mL water (Gretel Saß, personal communication). The solution was allowed to mix for approximately 4 h before lyophilizing. In some NMR experiments, the mannitol concentration was varied as indicated.

NMR

NMR experiments were performed by using a Bruker Avance 500 MHz NMR spectrometer. ^{1}H and $^{13}C\{^{1}H\}$ NMR experiments were performed; water suppression was implemented in the ^{1}H experiments to suppress the residual solvent peak. All samples were prepared in 740 μL D_2O with 10 μL DMSO for referencing, and performed at room temperature, samples were ~15 mM in Ti, and the pH of the solutions was 3.4.

Mass spectrometry

Mass spectrometry experiments used a Bruker (Billerica, MA) 9.4 Tesla Apex-Qe Hybrid Fourier Transform Ion Cyclotron Resonance (FT-ICR) mass spectrometer with an Apollo II electrospray ionization source. The instrument (running Compass Software with APEX control acquisition component (v.1.2) was set up to acquire single FID (512 K) data and with a mass range (m/z) from 100 to 2000. MKT4 was dissolved in water with no other additives and injected onto the instrument immediately. Bruker Daltonics DataAnalysis software (v. 3.4) was utilized for data analysis and assignments were based on exact mass measurements and fit to theoretical isotopic patterns (IsotopePattern algorithm, Bruker). Data were zero filled and Fourier transformed. Magnitude calculations generated each m/z mass spectrum.

pH titration

A stock solution of MKT4 or TDC (60 μM in Ti) was prepared. Aliquots were removed and adjusted to the desired pH (3–9) by using 0.10 M NaOH or 0.10 M HCl. UV/vis absorbance was measured within 30 min. Dilution was accounted for. A titration was also performed with the corresponding concentration of mannitol alone (420 μM) from the MKT4 titration. No significant absorbance above 200 nm was seen for mannitol in the absence of Ti. Speciation of this data was modeled by using Specfit/32™ global analysis software (Spectrum Software Associates, Chapel Hill, North Carolina).[47–50]

Calculations

All electronic structure calculations were carried out by using Gaussian 09.[51] The B3LYP exchange correlation functional with unrestricted Hartree–Fock wave functions (UB3LYP) determined ground state configurations for MKT4, TDC and various hydrolysis products. Minimum energy configurations were obtained by using a mixed basis set with LANL2DZ for the Ti and 6-31G+(d,p) for all other atoms. UV/vis predictions were carried out using time dependent DFT with a mixed basis set with LANL2DZ for the Ti and 6-31G(d) for all other atoms.

Titanium transferrin interactions

Transferrin binding. Transferrin was dissolved in 50 mM HEPES buffer (pH 7.4) with 0.1 M NaCl, 4 mM Na_3PO_4, and 20 mM $NaHCO_3$. Transferrin concentrations were determined by A_{280} ($\varepsilon = 93\,000\ M^{-1}\ cm^{-1}$).[52,53] A 600 μM stock solution of the Ti sources was prepared in solution conditions including 10% DMSO (TDC_{DMSO} or $MKT4_{DMSO}$), 50 mM malate buffer (pH 3.5) (TDC_{mal} or $MKT4_{mal}$),[17–20] 50 mM HEPES buffer (pH 7.4) ($MKT4_{HEPES}$), or water (TDC_{water}). TDC undergoes rapid precipitation in HEPES

buffer at pH 7.4, so a TDC_{HEPES} sample could not be made. Samples were prepared in Ti : Tf mole ratios varying from 0.0 to 4.0 with 50 μM Tf and up to 200 μM Ti. Samples were all brought to constant volume with buffer and the solution was allowed to equilibrate for 3 h before the UV/vis spectrum was measured. The pH of the samples was confirmed to be 7.4 after equilibration.

Fluorescence quenching. Protein and metal reagent stock solutions were prepared as described above, including $MKT4_{HEPES}$, $MKT4_{mal}$, TDC_{water}, and TDC_{mal}. $Fe(NTA)_2$ was prepared *in situ* from 10 mM $FeCl_3 \cdot 6H_2O$ and 30 mM nitrilotriacetic acid in water and then diluted with buffer. Final concentrations of 25 μM Tf and 250 μM metal were used, and samples were allowed to equilibrate for 3 h before measurements were made. The absorbance of the samples was checked to verify that the protein was loaded with metal. Samples were excited at 280 nm and fluorescence was measured from 300–400 nm with slit widths of 1.5 nm for both excitation and emission. Data were collected in triplicate and averaged.

Transferrin kinetics. Protein and metal reagent stock solutions were prepared as above. Samples were combined in a quartz cuvette to give a final Tf concentration of 12.5 μM and a Ti concentration of 250 μM, and scanning began within 10 s of mixing. Data were measured for 2 h at 30 s intervals at room temperature, and were collected in triplicate. The dilution of $MKT4_{mal}$ and TDC_{DMSO} into 50 mM HEPES buffer (pH 7.4) was performed to monitor the change in absorbance of the Ti starting materials upon pH equilibration. Finally, MKT4 in malate buffer which had been adjusted to pH 7.5 was added to Tf and monitored as previously described. Spectra were fit by using Specfit/32™ global analysis software (Spectrum Software Associates, Chapel Hill, North Carolina).[47–50] Factor analysis was used to determine the number of species contributing to the spectra. Where needed, initial fits of the data used fixed spectra of known components to determine a reasonable starting model. These rate constants were then used as the starting values for fitting the data without using the fixed spectral components. All reported fits were determined with all values freely floating.

Results

MKT4 characterization

MKT4 was prepared according to the patent.[21] While the patent covers metallocene formulation with several polyols, MKT4 was confirmed to be the titanocene–mannitol complex (Gretel Saß, personal communication), which has been tested for cytotoxicity against multiple cell lines.[42,44,45] ^1H NMR of MKT4 agreed with the previously reported values.[42] MKT4 is usually depicted as a monomeric species having a mannitol replacing the TDC chloride ligands, which are lost under the conditions of formulation.[22,45]

Proton NMR of MKT4 (as prepared, pH 3.4) with 7 equiv of mannitol showed a singlet for the cyclopentadienyl ring protons at 6.47 ppm (Fig S1, ESI†). A second small peak in the aromatic region also appears in the TDC spectrum. This species appears to be from the hydrolysis of the chloride ligands probably to make an oxo or hydroxo complex, without hydrolysis of the Cp rings. The region from 3–4 ppm shows peaks that agree with those of free mannitol, which is expected from the seven fold excess of mannitol in MKT4.

Proton decoupled carbon NMR spectra of MKT4 and related compounds were measured (Fig. 1). The MKT4 used in the clinical trials had a 7 : 1 ratio of mannitol to Ti; varying ratios of mannitol to Ti were used to probe the effect on mannitol binding to Ti. The aromatic region shows a sharp peak between 118 and 119 ppm (R1), and a broader peak between 119 and 122 ppm (R2). The R1 peak in the TDC spectrum shifts as much as 0.15 ppm downfield and decreases in intensity with increasing mannitol concentrations. The R2 peak in the TDC sample shows much larger shifts throughout the concentration range with a maximal shift of 1.08 ppm upfield.

The ^{13}C mannitol peaks were less affected by Ti binding. Maximal shifts for all three carbon peaks were seen in the 1 : 1 MKT4 sample. All the peaks shift upfield in the 1 : 1 MKT4 sample and move downfield with the increasing ratio of mannitol in the formulation. The terminal carbons (M1) show a total shift of 0.26 ppm, while the second and fifth carbons (M2) have a total shift of 0.18 ppm and the third and fourth carbons (M3) have shifts of 0.23 ppm. These differences in shifts may give some insight into

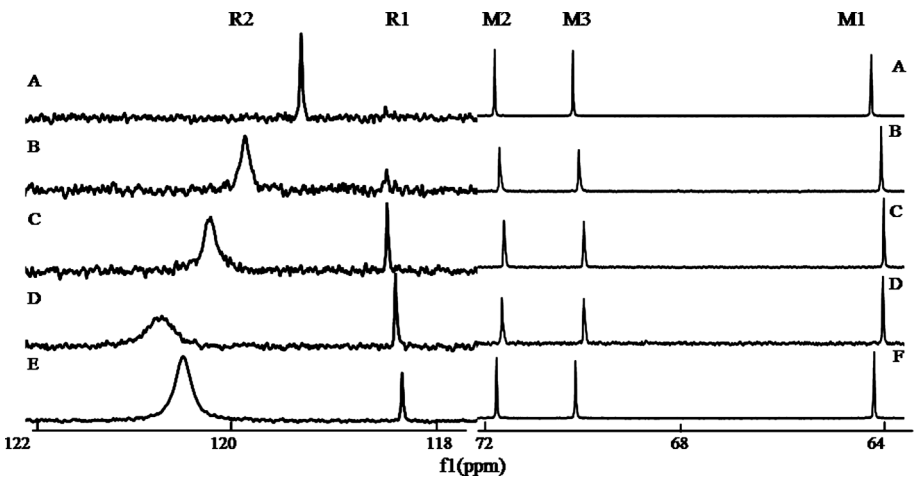

Fig. 1 $^{13}C\{^1H\}$ NMR of MKT4 and related compounds in D_2O at room temperature. A. 70 : 1 mannitol : titanium B. 7 : 1 mannitol : titanium C. 5 : 1 mannitol : titanium D. 1 : 1 mannitol : titanium E. TDC F. mannitol. Samples were approximately 60 μM in Ti.

the preferred binding site of the Ti center on the mannitol; the greatest interaction with Ti is indicated at the terminal mannitol position, and rapid exchange is indicated. Variable temperature NMR was attempted to resolve fluxional species, but no useful changes were seen in the operable temperature range.

FT-ICR mass spectrometry of MKT4 was performed; species containing Ti were evident by their characteristic isotope pattern. A Ti-containing peak at 359.10 *m/z* was observed, consistent with a doubly deprotonated mannitol bound to the titanocene, $[Cp_2Ti(C_6H_{13}O_6)]^+$, the predicted active species of MKT4 (Fig. 2). Other signals were observed for apparently hydrolyzed Ti complexes. These include a feature at 389.05 *m/z*, which agrees with the predicted mass for $[(Cp_2Ti)_2(\mu\text{-}O)(\mu\text{-}OH)]^+$. Another signal with a Ti isotope pattern was observed at 341.01 *m/z*. This feature agrees well with the predicted pattern for $[(Cp_2Ti)(CpTi(OH_2))(\mu\text{-}O)]^+$. No evidence for these oxo-bridged species was seen in the IR at the expected ~750 cm^{-1} (data not shown).[54]

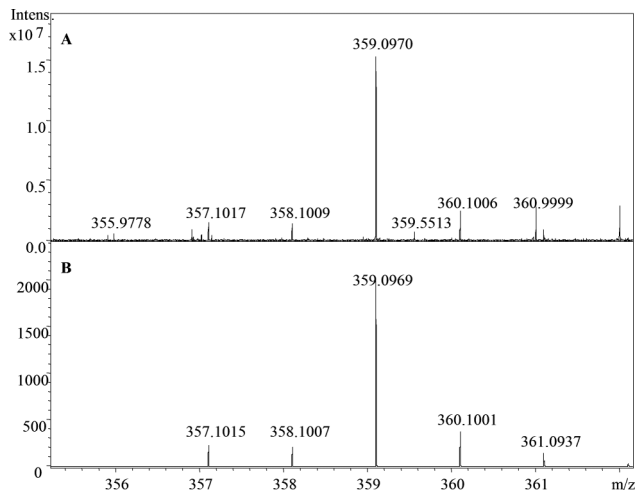

Fig. 2 FT-ICR MS spectrum showing a peak at 359.10 *m/z*. A, experimental spectra. B, simulated isotope pattern for $TiC_{16}H_{23}O_6^+$. MKT4 was dissolved in water and the spectrum was immediately measured.

The pH dependent speciation of MKT4 and TDC were studied by using UV/vis absorbance (Fig. 3 and Fig S2, ESI†). The overall changes in spectra and speciation were very similar. UV/vis spectra of the samples showed a large peak at 240 nm, which decreased and shifted to 230 nm with increasing pH. Around pH 5, the sample visibly clouded, which was seen in the spectra as an increased baseline near this pH range, but above pH 5 to 6 the cloudiness subsided. The apparent molar absorptivities of the TDC species all were lower than those of the MKT4 species, and the cloudiness observed between pH 5 and 6 did not fully reverse at higher pH values. Modeling of the data in SPECFIT/32 indicated three species in the pH range studied for both MKT4 and TDC. In the case of MKT4, the deprotonations occurred with $pK_{a1} = 4.6$ and $pK_{a2} = 6.3$. Small differences were seen in the TDC speciation, and the pK_a values were determined to be 4.5 and 6.3.

DFT calculations were performed on several potential MKT4 structures as well as on several possible hydrolyzed species (Fig. 4 and Fig S3, ESI†). The geometries of all pseudo-tetrahedral binding modes with mannitol bound to Ti through two oxygen atoms (**1–9**) were optimized. Hydroxide-bound species (**10–12**) were modeled and optimized with a singly bound mannitol. Each

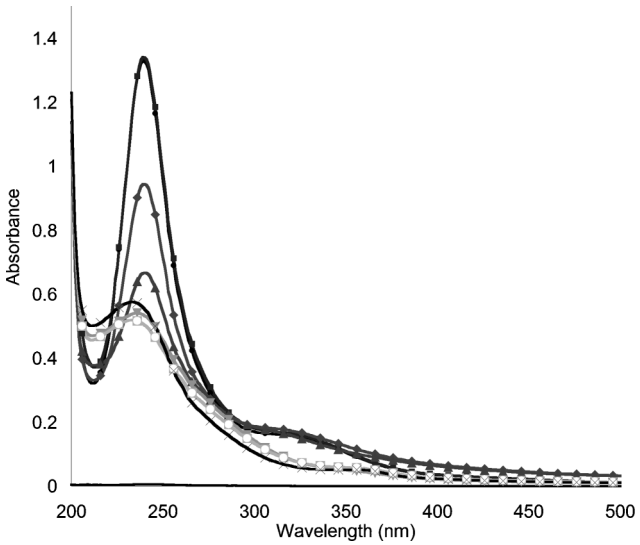

Fig. 3 MKT4 batch titration, pH values were: 3.12 (●), 4.20 (■), 4.99(◆), 5.94(▲), 7.30 (▼), 7.97 (◘) and 9.03 (×). Samples were 60 μM in Ti, and had 0.10 M NaCl. The pH was adjusted using 0.10 M KOH or 0.10 M HCl.

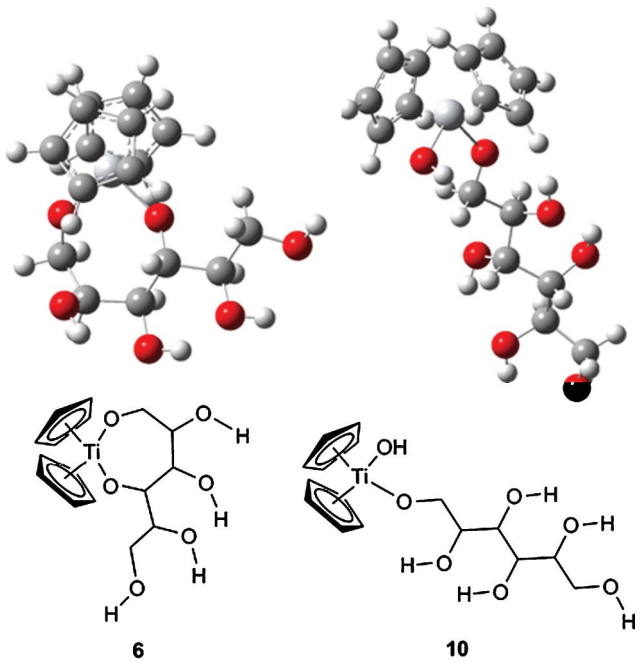

Fig. 4 Modeled structures of the lowest energy MKT4 isomers. Structure **6** has mannitol bound through two hydroxides. Structure **10** has one bond to mannitol and one hydroxide bound.

energy was reported in reference to its lowest energy isomer. The lowest energy species, **6**, was determined to be a seven membered ring bound at the 1 and 4 hydroxyls of the mannitol. The optimized geometry had a hydrogen bond between the proton of the 2 hydroxyl and the oxygen of the 3 hydroxyl, which gives this conformation a higher stability. The energies of the unhydrolyzed species had a maximal difference of 10.4 kcal mol^{-1}, which was for species **3**, which had mannitol bound at the 3 and 4 positions of the mannitol, creating a five membered ring.

The hydroxide bound species (**10–12**) had a range in energies of 2.7 kcal mol^{-1}. The most stable conformation was structure **10** in

which the Ti is bound by the terminal hydroxyl of the mannitol and the second open binding site is occupied by an hydroxide. Calculations of the trajectory of formation of these species from the two site bound mannitol species (**1–9**) were computed, and all reactions were favored to form the hydrolyzed species. Evidence for hydrolysis products of this form was not seen in the mass spec data. The energetics of further hydrolysis of these species to form $Cp_2Ti(OH)_2$ was also determined and found to be favorable in all cases, though by only a maximum of 3.4 kcal mol^{-1}. Values for these reactions are listed in the ESI.† Corresponding titanyl and water bound species failed to optimize to reasonable structures.

In addition to energy optimizations of these species, the UV/vis spectra were calculated. The predicted UV/vis spectra were reasonably well matched with the observed spectra in the batch titrations, showing similar trends in absorbance shifts with increasing hydrolysis. Species **1–9** showed maximum absorbances between 300 and 335 nm, agreeing well with the low pH species, while species **10–12** had maximum absorbances between 290 nm and 310 nm, agreeing well with the higher pH species.

Titanium transferrin interactions

Transferrin binding. The binding of TDC and MKT4 to human serum Tf were monitored by following the absorbance of the complex. This peak at 321 nm corresponds to a tyrosine to Ti charge transfer band in the Tf metal binding site.[24]

MKT4 binding to Tf was studied in a variety of buffer conditions (including Tris, HEPES and phosphate) with particular focus on MKT4 reconstituted in a pH 3.5, 50 mM malate buffer ($MKT4_{mal}$), the buffer that MKT4 was prepared in for the clinical trials.[17–20] Equivalent results were seen for binding across this range of buffers. In the presence of malate, both MKT4 and TDC showed a shift in the absorbance at 321 nm to a λ_{max} at 333 nm (Fig. 5); this suggests that malate acts as a synergistic anion for binding.[55]

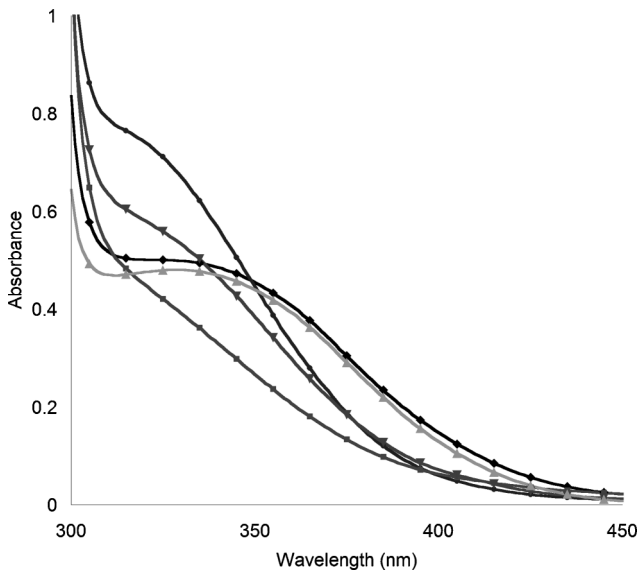

Fig. 5 Synergistic anion comparison of titanium transferrin binding. When malate is the synergistic anion, there is a shift in the tyrosine to titanium charge transfer to 333 nm. $MKT4_{mal}$ (◆), $MKT4_{DMSO}$ (●), $MKT4_{HEPES}$ (■), TDC_{DMSO} (▼), TDC_{mal} (▲). Spectra are of 50 μM Tf in HEPES buffer with at least a 4 fold excess of Ti.

Transferrin loaded with Ti from $MKT4_{DMSO}$ had a molar absorptivity of 7500 M^{-1} cm^{-1} per site with a λ_{max} at 321 nm, while the A_{333} for $MKT4_{mal}$ had an apparent molar absorptivity of 5000 M^{-1} cm^{-1} per site (Fig. 6). Binding titrations performed under both these buffer conditions for MKT4 showed saturation with approximately two equiv of Ti(IV). TDC_{DMSO} and TDC_{water} binding was also monitored and matched well with the findings of Sadler *et al.* (Fig S5, ESI†).[25] TDC_{mal} binding was very similar to $MKT4_{mal}$ binding, with a molar absorptivity of 5000 M^{-1} cm^{-1} per Tf binding site.

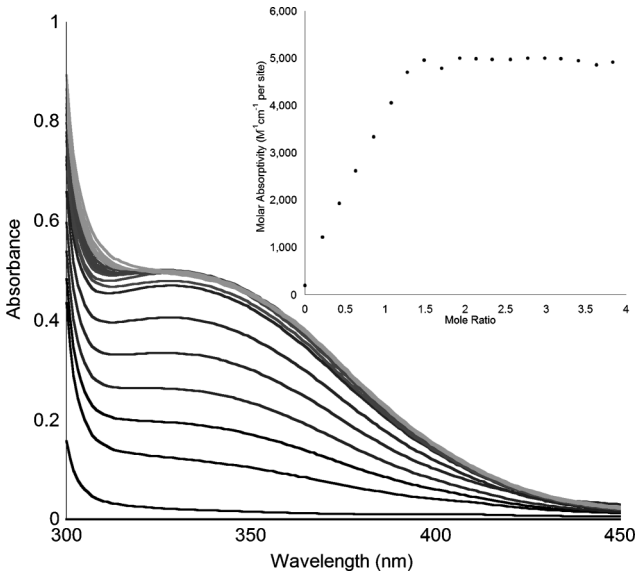

Fig. 6 $MKT4_{mal}$ Tf binding. Tf was held at 50 μM and the MKT4 ratio was varied from 0.0 to 4.0 molar equivalents. Inset is the A_{333nm} for binding. Binding saturation is seen slightly below two equivalents of titanium.

Fluorescence quenching

Binding of Ti(IV) to Tf was also monitored by fluorescence. Transferrin fluorescence is often used as a measure of lobe closure upon binding, as some of the quenching is caused by the change in the local environment of the tryptophan residues.[56,57] Transferrin quenching by $MKT4_{HEPES}$ and $MKT4_{mal}$ was measured. Quenching was comparable between the two buffer conditions. TDC-induced quenching was monitored for TDC_{mal} and TDC_{water}; malate increased quenching. This enhanced quenching with malate buffer further supports the idea that malate acts as the synergistic anion for binding under these conditions. Titanocene dichloride showed increased quenching compared to MKT4 under both sets of buffer conditions (Fig S6, ESI†, and Table 2).

Table 2 Fluorescence quenching data, relative to apo-Tf fluorescence. A 5 fold excess of metal was added to 25 μM Tf in HEPES buffer. Experiments were performed in triplicate and average values are reported

	% Fluorescence	% Quenching	Standard Deviation
$Fe(NTA)_2$	20.3	80.2	1.0
$MKT4_{HEPES}$	32.0	68.0	6.4
$MKT4_{mal}$	39.2	61.7	3.2
TDC_{water}	33.3	67.9	2.3
TDC_{mal}	21.2	79.6	1.6

Table 3 Rate constants for the kinetic fits of Tf binding as determined in SPECFIT/32. Rates are listed in min^{-1}. 2 h kinetics experiments were performed in triplicate and rate constants reported are averages. Errors reported for the $MKT4_{mal}$ pH 7.5 data are the error of fit parameters for one experiment

	TDC_{DMSO} 2 h	$MKT4_{mal}$ 2 h	$MKT4_{mal}$ pH 7.5
k_1	1.07 ± 0.14	0.681 ± 0.652	1.99 ± 0.11
k_2	0.145 ± 0.008	0.081 ± 0.029	0.091 ± 0.003
k_3	0.051 ± 0.001	0.020 ± 0.008	

Transferrin kinetics

Binding of MKT4 and TDC to Tf was monitored by UV/vis spectroscopy. $MKT4_{mal}$ kinetics were monitored with a tenfold excess of MKT4 to Tf binding sites. The pH of the final solution was verified to be 7.4. A slow decrease in absorbance was observed that was dominated by the absorbance change of MKT4 alone during equilibration from pH 3.5 to pH 7.4 (Fig S7, ESI†), by comparison to control experiments in which the absorbance of $MKT4_{mal}$ was monitored upon mixing with HEPES (pH 7.4). These absorbance changes matched well with the conversion of the low pH MKT4 species to the high pH species (data not shown). The data fit well to a sequential three step model (Fig S8, ESI†). The first two species (very similar in absorbance, each with a peak near 320 nm) were gone within fifteen min with rate constants of 0.68 and 0.081 min^{-1} respectively. The third species has a decreased absorbance at 320 nm, and a shift towards 350 nm; this peak further shifts towards 350 nm with $k_3 = 0.02$ min^{-1} as it forms the final species. A slow, low intensity increase was caused by precipitation in longer experiments (Fig S9, ESI†).

TDC, as in the preclinical trials, was prepared in a 10% DMSO solution (Fig S10, ESI†). The species were similar to those observed for $MKT4_{mal}$, with somewhat increased rates (Table 3, Fig S11, ESI†). Overnight experiments required invocation of a fifth species because of precipitation of the excess TDC (Fig S12, ESI†).

In order to separate the $MKT4_{mal}$ binding to Tf from the rather slow pH equilibration of the Ti starting materials into the pH 7.4 buffer masking it, MKT4 in malate buffer was adjusted to pH 7.5 and then added to Tf (Fig. 7). These binding data were analyzed and showed a sequential two step model with rate constants k_1 = 1.99 min^{-1} and k_2 = 0.091 min^{-1}. The initial Ti Tf binding step appears to be unresolved under the experimental conditions, so the initial species appears to already have Ti within ~10 s. The final species matches well with the $MKT4_{mal}$ species determined in the thermodynamic experiments (Fig S13, ESI†). A similar experiment with the corresponding higher pH TDC_{DMSO} species could not be performed because TDC immediately precipitates under these conditions.

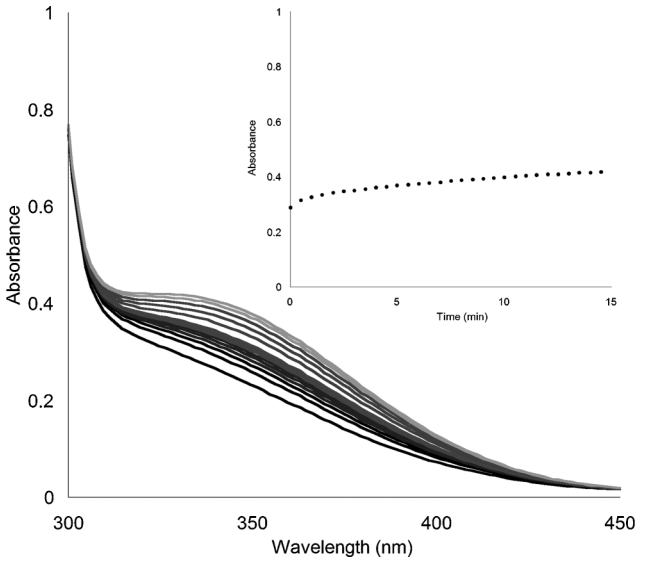

Fig. 7 $MKT4_{mal}$ (pH 7.5) Tf binding. A 20 fold molar excess of $MKT4_{mal}$ preadjusted to pH 7.5 was added to 12.5 μM Tf in HEPES buffer in order to separate the absorbance changes due to metal binding from those due to pH equilibration. Inset is the A_{333nm} for binding.

Discussion

MKT4 characterization

The MKT4 formulation likely gives several products that are in rapid equilibrium in solution. With excess mannitol, there is exchange of bound and free mannitol on the Ti center. Interconversion among multiple binding sites on the mannitol is also likely, as supported by the NMR data. The Cp carbon resonances are sensitive to the presence of mannitol, and support this model. The higher field peaks corresponding to the carbon atoms of mannitol show very little shift with increasing Ti concentrations. Because of the fluxional nature of the titanocene–mannitol interaction in this complex, at low mannitol to Ti ratios no individual mannitol is strongly affected by the Ti center. In addition to exchange between mannitol molecules, movement between different binding sites on the mannitol would minimize the shift seen in the mannitol peaks. As the mannitol concentration increases, the free mannitol is in much greater concentration than the bound mannitol, and diminishes the peak shift of the mannitol carbons. The greatest shifts in the spectra were observed for the terminal carbons of the mannitol (M1). This result suggests that the hydroxides on the M1 carbons are slightly preferentially bound by the Ti. This model matches well with the energy optimization calculations in which the preferred hydroxide bound species, **10**, is bound at the M1 position, and the lowest energy doubly bound mannitol species, **6**, is bound at the M1 and M3 positions.

Mannitol binding was confirmed by using mass spectrometry. A Ti-containing peak was observed at m/z = 359.10 which is consistent with the mass of $[Cp_2Ti(C_6H_{12}O_6)H]^+$; a species in which both chlorides have been lost from TDC and one mannitol is bound to the Ti. Other peaks with the Ti isotope pattern corresponded to complexes that contained two Ti atoms with bridging oxygens. No evidence for these species was seen in IR experiments, and including them in the solution speciation models did not improve the fits; whether they are gas phase reaction products or they exist as minor products in solution is unknown.

DFT calculations were performed to evaluate different binding modes of mannitol to the titanocene moiety. The first set of calculations focused on the configurations for mannitol when bound through two hydroxyl groups (the form most often invoked for MKT4). Geometry optimizations of all the permutations of

this binding mode were performed. The lowest energy structure, **6**, featured a seven membered ring stabilized by a hydrogen bond between two of the hydroxyls of the mannitol. The highest energy structure, **3**, was a five membered ring with no apparent hydrogen bonds. The other structures segregated into two groups, including three structures with energies less than 4.1 kcal mol^{-1} above **6** and four structures with energies more than 7.1 kcal mol^{-1} above **6**. The lower energy configurations have hydroxyl groups on the mannitol aligned properly to afford an intramolecular hydrogen bond. The higher energy configurations have hydroxyl groups which are not aligned properly for intramolecular hydrogen bonds. The energy differences between the species should be further suppressed in solution, as hydrogen bonds will readily form between water and the hydroxyls of the mannitol. These data support the existence of a mixture of these species in solution, without any one species being energetically favored.

One possible mechanism for interconversion among these species is an associative mechanism in which a water binds to the Ti, resulting in a monodentate mannitol and an aqua ligand. In order to test this model computationally, optimizations of the water-bound MKT4 species with one mannitol were attempted. All structures of this form optimized to a $[Cp_2Ti(C_6H_{13}O_6)]^+ \cdot H_2O$ species, rather than the expected structure. This observation may be because a bound water would readily hydrolyze to an hydroxide or oxide on the Ti(IV). The hydroxide bound structures were optimized (structures **10–12**) and the reaction energy for their formation from MKT4 hydrolysis was determined (Table S1, ESI†). The energies between these three structures had a total difference of 2.7 kcal mol^{-1}, a fairly small energy difference. Attempts to assess further hydrolyzed species failed to minimize to reasonable species.

Reaction energies were calculated for the formation of **10–12** from the MKT4 conformations **1–9**. Formation of the hydroxido species from the two site bound mannitol species and water was found in all cases to be favorable. Further hydrolysis of these compounds to $Cp_2Ti(OH)_2$ was also determined to be favored under the conditions of the calculations. However, the NMR and mass spectrometry data support the existence of a mannitol bound species in experiment, so the excess mannitol in the experimental conditions likely hinders some of this hydrolysis.

When MKT4 and TDC are dissolved in water, the pH of the solution decreases significantly, which is likely due to initial rapid hydrolysis steps. TDC requires this lowered pH in order to dissolve; at pH 7.4, TDC is not soluble. MKT4 dissolves in buffered solutions at pH 7.4, but has a reduced solubility near pH 5. Near pH 5 and 6, precipitation of both TDC and MKT4 was observed. Precipitant was persistent in the TDC samples, but in MKT4, neutral and basic solutions allowed the reagent to redissolve. The stability at higher pH values may be due to better mannitol binding. NMR and mass spectrometry attempts in higher pH solutions did not show significant differences from the low pH MKT4 data (data not shown).

The speciation of MKT4 and TDC were both determined. MKT4 underwent two deprotonation events with $pK_{a1} = 4.6$ and $pK_{a2} = 6.3$. In assigning possible species to these, it seems likely that the mid-pH species, from which precipitation is observed, is a neutral species. One possibility for this would be the mannitol bound by two hydroxides (**1–9**), indicating that the lower pH species is a less hydrolyzed form, perhaps with a coordinated water, and the higher pH species would be further hydrolyzed, giving charged, more soluble species.

From the UV/vis prediction calculations, it is unsurprising that the spectra of TDC and MKT4 are similar, as most of the transitions appear to originate from Cp to Ti charge transfers. The oxygen ligands derived from water or mannitol do not appear to make significant changes to the electronics surrounding the Ti center (Fig S4, ESI†).

MKT4 at low pH is likely a mixture of the calculated structures **1–9** with no strong preference for any particular binding mode. The high mannitol concentration in the formulation gives a greater stability to the Ti center to resist hydrolysis as seen in the NMR experiments. Fitting of the pH speciation indicates that mannitol binding is favored at higher pH values, and it is likely that in plasma, after clinical administration, MKT4 exists in a mannitol bound form.

Titanium transferrin studies

Transferrin binding. Transferrin binding studies were performed with MKT4 reconstituted in 50 mM malate buffer at pH 3.5, to mimic the conditions of administration in the clinical trials. Binding resulted in a shift to 333 nm in the tyrosine to Ti(IV) charge transfer band seen with TDC and Ti citrate at 321 nm. This result was also seen when TDC was delivered in malate buffered solutions. This shift in λ_{max} indicates that malate acts as a synergistic anion for Ti(IV) binding, as it does for Fe(III) binding.[55] The molar absorptivity is approximately the same for both Ti sources in the presence of malate. This similarity in binding does not hold when the synergistic anion is carbonate. Transferrin-bound Ti delivered as $MKT4_{DMSO}$ has a much higher molar absorptivity than that delivered as TDC_{DMSO}. This difference in molar absorptivities suggests differences in the state of hydrolysis of the bound Ti.

Saturation of Ti binding to Tf was determined by adding Ti to Tf from 0.0 to 4.0 mole equivalents. MKT4 was added in malate buffer, and showed binding saturation at approximately two equiv, as expected. The molar absorptivity for this complex (at 333 nm) was 5000 M^{-1} cm^{-1} per site. For samples of MKT4 delivered in HEPES buffer at pH 7.4, saturation was not observed under the conditions of the experiment (data not shown), but in conjunction with the kinetics studies, the final complex had a molar absorptivity of 7500 M^{-1} cm^{-1} per site. This result suggests that MKT4 binds in the same state whether delivered in 10% DMSO or pH 7.4 buffer. Transferrin bound two equiv of Ti from TDC with $\varepsilon \sim 2500$ M^{-1} cm^{-1} per site. MKT4 had no significant absorbance at 321 nm or 333 nm.

Iron binding to Tf quenches its intrinsic fluorescence through lobe closure and electronic effects on tryptophan residues near the metal binding sites.[56,57] Titanium citrate quenches Tf fluorescence to 27% of its original fluorescence.[41] Fluorescence quenching of Tf with MKT4 in malate and HEPES buffer as well as TDC in both malate buffer and water was measured to determine the effect of Ti source and buffer conditions on fluorescence (Table 2). MKT4 in malate was nearly twenty percent less quenching than TDC in malate. These variations indicate a difference in hydrolysis state of the bound Ti or differences in the state of lobe closure of the Tf. The increased Tf quenching seen for TDC binding compared to MKT4 binding highlights that changes observed in the absorbance

and fluorescence of Ti bound Tf report on different phenomena. MKT4 and TDC likely bind in different states of hydrolysis and with different lobe closure.

The differences in fluorescence quenching between the malate containing samples and their malate free counterparts also support the finding that malate is acting as a synergistic anion. MKT4 showed decreased quenching with malate over HEPES. The difference between the values was small and nearly within error. Greater differences were seen between TDC with and without malate. A nearly ten percent increase in quenching was seen for TDC binding in malate.

Transferrin kinetics

Initial spectra in experiments with $MKT4_{mal}$ and TDC_{DMSO} had high absorbances due to the low pH Ti species present. These data fit best to a sequential three step model, in which pH equilibration precedes protein interaction. The determined species matched well with the species seen in the pH titration, indicating that the Ti-to-Tf binding follows and is greatly masked both kinetically and optically by the pH equilibration of the Ti starting material.

To try to separate these processes, MKT4 was reconstituted in higher pH malate buffer (pH 7.5), to minimize absorbance changes from pH equilibration of the MKT4. These data fit well to two sequential steps with apparent rate constants, $k_1 = 1.99\ min^{-1}$ and $k_2 = 0.09\ min^{-1}$. These rate constants are similar in magnitude to those observed for the $MKT4_{mal}$ and TDC_{DMSO} experiments. The corresponding TDC experiment with neutral pH TDC could not be performed due to the insolubility of TDC at pH 7.4.

When these results are considered in light of the cytotoxicity data for the different Ti sources, it seems that weak Ti binding to Tf may be needed for increased cytotoxicity. Whether this effect is because Tf is not a carrier for the active fraction of Ti, but instead is a competitor, or because productive release of Ti from Tf requires somewhat weaker binding, remains to be determined. In Köpf and Köpf-Maier's *in vitro* studies, TDC showed high activity, but did not show the same promise in clinical trials. This difference is more understandable when MKT4 is considered as a different compound; its lack of activity was seen both *in vitro* (Table 1), and *in vivo* in the clinical trials based on its increased binding to Tf. Titanium citrate shows little to no cytotoxic activity and is rapid and effective at delivering Ti to Tf.

Conclusions

The ligand environment of Ti plays a large role in its interactions in serum. The mannitol in the formulation of MKT4 stabilizes TDC from hydrolysis, and forms a mixture of species which are in rapid equilibrium. No one binding mode of mannitol was judged to be significantly more stable than another. The interaction of mannitol with the titanocene center increases the stability of the complex in high pH solutions and also renders it soluble in near neutral pH solutions.

The formulation of Ti has an effect on its binding to Tf. Inclusion of malate in the buffer affects the tyrosine to Ti charge transfer, likely because malate is acting as a synergistic anion. MKT4 has a higher molar absorptivity when bound to Tf than TDC does, and in light of the Ti citrate binding data, this difference may be caused by a difference in the binding state of the Ti, perhaps in the hydrolysis state of the bound Ti. TDC shows an increased quenching of Tf fluorescence over MKT4, which also indicates differences in Ti binding, perhaps in changes in lobe closure. This result reinforces that absorbance and fluorescence changes report on different aspects of metal binding to Tf. When these titanium reagents are introduced in their low-pH formulations to Tf, slow pH equilibration masks protein binding. When the differences in binding between the Ti sources studied by these methods are considered together, it seems that there may be a correlation between weak titanium–transferrin interactions and anticancer activity.

Acknowledgements

We thank the American Cancer Society Research Scholar Grant RSG-06-246-01-CDD for funding this research. V.S.B. acknowledges support from NSF ECCS-040419. We thank Professor Nilay Hazari for helpful discussions. This work was supported in part by the Yale University Faculty of Arts and Sciences High Performance Computing facility. We thank the Keck Center at Yale for help with the mass spectral data.

Notes and references

1 H. Köpf and P. Köpf-maier, *Angew. Chem., Int. Ed. Engl.*, 1979, **18**, 477–478.
2 P. Köpf-maier and H. Köpf, *Naturwissenschaften*, 1980, **67**, 415–416.
3 P. Köpf-maier, A. Moormann and H. Köpf, *Eur. J. Cancer Clin. Oncol.*, 1985, **21**, 853–857.
4 P. Köpf-maier, F. Preiss, T. Marx, T. Klapotke and H. Köpf, *Anticancer Res.*, 1986, **6**, 33–38.
5 P. Köpf-maier and H. Köpf, *Arzneimittelforschung*, 1987, **37**, 532–534.
6 J. R. Boyles, Master of Science thesis, Queen's University, Kingston, Ontario, Canada, 1997.
7 P. Köpf-Maier, *Anticancer Res.*, 1999, **19**, 493–504.
8 M. M. Harding and G. Mokdsi, *Curr. Med. Chem.*, 2000, **7**, 1289–1303.
9 E. Melendez, *Crit. Rev. Oncol. Hematol.*, 2002, **42**, 309–315.
10 F. Caruso and M. Rossi, in *Metal Ions in Biological Systems, Vol 42: Metal Complexes in Tumor Diagnosis and as Anticancer Agents*, 2004, pp. 353–384.
11 F. Caruso and M. Rossi, *Mini-Rev. Med. Chem.*, 2004, **4**, 49–60.
12 P. M. Abeysinghe and M. M. Harding, *Dalton Trans.*, 2007, 3474–3482.
13 J. H. Bannon, I. Fichtner, A. O'Neill, C. Pampillon, N. J. Sweeney, K. Strohfeldt, R. W. Watson, M. Tacke and M. M. Mc Gee, *Br. J. Cancer*, 2007, **97**, 1234–1241.
14 U. Olszewski and G. Hamilton, *Anti-Cancer Agents Med. Chem.*, 2010, **10**, 302–311.
15 C. M. Kurbacher, P. Mallmann, J. A. Kurbacher, G. Sass, P. E. Andreotti, A. Rahmun, H. Hubner and D. Krebs, *Anticancer Res.*, 1994, **14**, 1961–1965.
16 C. V. Christodoulou, A. G. Eliopoulos, L. S. Young, L. Hodgkins, D. R. Ferry and D. J. Kerr, *Br. J. Cancer*, 1998, **77**, 2088–2097.
17 C. V. Christodoulou, D. R. Ferry, D. W. Fyfe, A. Young, J. Doran, T. M. T. Sheehan, A. Eliopoulos, K. Hale, J. Baumgart, G. Saß and D. J. Kerr, *J. Clin. Oncol.*, 1998, **16**, 2761–2769.
18 A. Korfel, M. E. Scheulen, H. J. Schmoll, O. Grundel, A. Harstrick, M. Knoche, L. M. Fels, M. Skorzec, F. Bach, J. Baumgart, G. Saß, S. Seeber, E. Thiel and W. E. Berdel, *Clin. Cancer Res.*, 1998, **4**, 2701–2708.
19 G. Lümmen, H. Sperling, H. Luboldt, T. Otto and H. Rübben, *Cancer Chemother. Pharmacol.*, 1998, **42**, 415–417.
20 N. Kröger, U. R. Kleeberg, K. Mross, L. Edler, G. Saß and D. K. Hossfeld, *Onkologie*, 2000, **23**, 60–62.
21 *US Pat.*, 5296237, 1994.
22 J. H. Toney and T. J. Marks, *J. Am. Chem. Soc.*, 1985, **107**, 947–953.
23 A. D. Tinoco, E. V. Eames and A. M. Valentine, *J. Am. Chem. Soc.*, 2008, **130**, 2262–2270.
24 H. Z. Sun, H. Y. Li, R. A. Weir and P. J. Sadler, *Angew. Chem., Int. Ed.*, 1998, **37**, 1577–1579.

25 M. L. Guo, H. Z. Sun, H. J. McArdle, L. Gambling and P. J. Sadler, *Biochemistry*, 2000, **39**, 10023–10033.
26 P. F. Lindley, in *Handbook of Metalloproteins*, ed. I. Bertini, Marcel Dekker, New York, Editon edn, 2001, vol. 1, pp. 793–811.
27 W. R. Harris, *Struct. Bonding*, 1998, **92**, 121–162.
28 K. Ishiwata, T. Ido, M. Monma, M. Murakami, H. Fukuda, M. Kameyama, K. Yamada, S. Endo, S. Yoshioka, T. Sato and T. Matsuzawa, *Int. J. Radiat. Appl. Instrum., Part A*, 1991, **42**, 707–712.
29 W. P. Faulk, B. L. Hsi and P. J. Stevens, *Lancet*, 1980, **316**, 390–392.
30 M. Panaccio, J. R. Zalcberg, C. H. Thompson, M. J. Leyden, J. R. Sullivan, M. Lichtenstein and I. F. C. McKenzie, *Immunol. Cell Biol.*, 1987, **65**, 461–472.
31 M. Cazzola, G. Bergamaschi, L. Dezza and P. Arosio, *Blood*, 1990, **75**, 1903–1919.
32 J. Williams and K. Moreton, *Biochem. J.*, 1980, **185**, 483–488.
33 E. Y. Tshuva and D. Peri, *Coord. Chem. Rev.*, 2009, **253**, 2098–2115.
34 L. Messori, P. Orioli, V. Banholzer, I. Pais and P. Zatta, *FEBS Lett.*, 1999, **442**, 157–161.
35 M. L. Guo and P. J. Sadler, *J. Chem. Soc., Dalton Trans.*, 2000, 7–9.
36 Y. Perez, V. Lopez, L. Rivera-Rivera, A. Cardona and E. Melendez, *JBIC, J. Biol. Inorg. Chem.*, 2005, **10**, 94–104.
37 A. D. Tinoco and A. M. Valentine, *J. Am. Chem. Soc.*, 2005, **127**, 11218–11219.
38 A. Cardona and E. Melendez, *Anal. Bioanal. Chem.*, 2006, **386**, 1689–1693.
39 L. M. Gao, R. Hernandez, J. Matta and E. Melendez, *JBIC, J. Biol. Inorg. Chem.*, 2007, **12**, 959–967.
40 A. Sarmiento-Gonzalez, J. R. Encinar, A. M. Cantarero-Roldan, J. M. Marchante-Gayon and A. Sanz-Medel, *Anal. Chem.*, 2008, **80**, 8702–8711.
41 A. D. Tinoco, C. D. Incarvito and A. M. Valentine, *J. Am. Chem. Soc.*, 2007, **129**, 3444–3454.
42 P. W. Causey, M. C. Baird and S. P. C. Cole, *Organometallics*, 2004, **23**, 4486–4494.
43 G. N. Kaluderovic, V. Tayurskaya, R. Paschke, S. Prashar, M. Fajardo and S. Gomez-Ruiz, *Appl. Organomet. Chem.*, 2010, **24**, 656–662.
44 G. D. Potter, M. C. Baird, M. Chan and S. P. C. Cole, *Inorg. Chem. Commun.*, 2006, **9**, 1114–1116.
45 G. D. Potter, M. C. Baird and S. P. C. Cole, *J. Organomet. Chem.*, 2007, **692**, 3508–3518.
46 M. Tacke, L. T. Allen, L. Cuffe, W. M. Gallagher, L. Ying, O. Mendoza, H. Muller-Bunz, F. J. K. Rehmann and N. Sweeney, *J. Organomet. Chem.*, 2004, **689**, 2242–2249.
47 H. Gampp, M. Maeder, C. J. Meyer and A. D. Zuberbuhler, *Talanta*, 1985, **32**, 251–264.
48 H. Gampp, M. Maeder, C. J. Meyer and A. D. Zuberbuhler, *Talanta*, 1985, **32**, 95–101.
49 H. Gampp, M. Maeder, C. J. Meyer and A. D. Zuberbuhler, *Talanta*, 1985, **32**, 1133–1139.
50 H. Gampp, M. Maeder, C. J. Meyer and A. D. Zuberbuhler, *Talanta*, 1986, **33**, 943–951.
51 M. J. Frisch, G. W. Trucks, H. B. Schlegel, G. E. Scuseria, M. A. Robb, J. R. Cheeseman, G. Scalmani, V. Barone, B. Mennucci, G. A. Petersson, H. Nakatsuji, M. Caricato, X. Li, H. P. Hratchian, A. F. Izmaylov, J. Bloino, G. Zheng, J. L. Sonnenberg, M. Hada, M. Ehara, K. Toyota, R. Fukuda, J. Hasegawa, M. Ishida, T. Nakajima, Y. Honda, O. Kitao, H. Nakai, T. Vreven, J. A. Montgomery, Jr., J. E. Peralta, F. Ogliaro, M. Bearpark, J. J. Heyd, E. Brothers, K. N. Kudin, V. N. Staroverov, R. Kobayashi, J. Normand, K. Raghavachari, A. Rendell, J. C. Burant, S. S. Iyengar, J. Tomasi, M. Cossi, N. Rega, J. M. Millam, M. Klene, J. E. Knox, J. B. Cross, V. Bakken, C. Adamo, J. Jaramillo, R. Gomperts, R. E. Stratmann, O. Yazyev, A. J. Austin, R. Cammi, C. Pomelli, J. Ochterski, R. L. Martin, K. Morokuma, V. G. Zakrzewski, G. A. Voth, P. Salvador, J. J. Dannenberg, S. Dapprich, A. D. Daniels, O. Farkas, J. B. Foresman, J. V. Ortiz, J. Cioslowski and D. J. Fox, *GAUSSIAN 09 (Revision A.2)*, Gaussian, Inc., Wallingford, CT, 2009.
52 N. D. Chasteen, *Coord. Chem. Rev.*, 1977, **22**, 1–36.
53 W. R. Harris and V. L. Pecoraro, *Biochemistry*, 1983, **22**, 292–299.
54 A. Bodner, P. Jeske, T. Weyhermuller, K. Wieghardt, E. Dubler, H. Schmalle and B. Nuber, *Inorg. Chem.*, 1992, **31**, 3737–3748.
55 M. R. Schlabach and G. W. Bates, *J. Biol. Chem.*, 1975, **250**, 2182–2188.
56 Q. Y. He, A. B. Mason, B. A. Lyons, B. M. Tam, V. Nguyen, R. T. A. MacGillivray and R. C. Woodworth, *Biochem. J.*, 2001, **354**, 423–429.
57 N. G. James, S. L. Byrne, A. N. Steere, V. C. Smith, R. T. A. MacGillivray and A. B. Mason, *Biochemistry*, 2009, **48**, 2858–2867.

